AN ABSTRACT OF THE THESIS OF

Nathan Sky Nebergall for the degree of Master of Science in Applied Physics presented on 08/17/2006
Title: Metallic Nano-Scale Conductors

Abstract approved: _____
William M. Hetherington III

A new, reproducible method of using electromigration to form metallic nano-conductors is developed using gold and a tin-silver alloy. Measurements revealed a quantization of the electrical conductance consistent with the theory of quantum conductance. The theory of quantum conductance is applied to show that a nano-conductor with a cross-section of only 12 or 13 atoms was created.

Master of Science thesis of Nathan Sky Nebergall
presented on August 17, 2006.

APPROVED:

_____
Major Professor, representing Applied Physics

_____
Chair of the Department of Physics

_____
Dean of the Graduate School

I understand that my thesis will become permanent collection of Oregon State University libraries. My signature below authorizes of my thesis to any reader upon request.

_____
Nathan Sky Nebergall

# METALLIC NANOSCALE CONDUCTORS

by
Nathan Sky Nebergall

A THESIS

submitted to

Oregon State University

in partial fulfillment of
the requirements for the
degree of

Master of Science

Presented August 17, 2006
Commencement June 2008

TABLE OF CONTENTS

LIST OF FIGURES

## 1) Introduction

Contemporary solid-state transistor technology functions by controlling the movement of large numbers of electrons through doped sections of bulk silicon. The speed of solid-state devices may be increased, by reducing the device size and therefore the distance that the electrons must travel. However, eventually the size of integrated circuits will be reduced to the point where physical limits of the technology will be reached.

When electronic components become small enough, on the scale of nanometers, new quantum mechanical properties must be taken into consideration. These properties include a quantization of the conductance and electron tunneling. In addition, the high current densities, within ultra-thin conductors, leads to localized heating and increased mobility, causing cavity and extrusion growth. To continue to improve electronics at historical rates a better understanding of the nano-scale electrodynamic properties of conductors will be required

The goal of this research project was to create stable, metallic nano-conductors and study the electrodynamic properties. A flex-structure nano-press system was developed to create the nano-scale conductors between bulk electrodes. The initial system functioned by bringing two sharpened gold wire tips into contact. Then, the contact is carefully pulled apart forming a break junction. Near the breaking point the contact may consist of only a few atoms and is a nano-scale conductor between two bulk electrodes. A constant bias potential is applied across the contact during the process and the resulting current is measured as a function of time. Using the potential and current measurements, the conductance and the cross section size of the conductor may be inferred. The experiments

showed the successful formation of both gold and tin-silver alloy nano-conductors with properties consistent with the theory of quantum conduction.

The instrumentation was greatly improved by replacing the wire tips with electrode blades. Later experiments with this system used electromigration, or the movement of atoms in an electrical current to grow a nanoscale conduction bridge between the electrode blades. The nano-conductors formed with electromigration appeared stable on a time scale of minutes. The data indicates that these conductors have waists as narrow as 12 atoms.

The electrical properties of the bridges were studied using multi-meters and the electrical and spatial data was recorded by hand. Although excellent data was generated, during conductor formation, it was observed that additional dynamics were occurring at faster time scales and a new, faster data acquisition was needed.

The final phase of the project was to design a new high-speed data acquisition and control system to record the high-speed dynamics. The system is designed to rapidly scan the nano-contact as a function of position and bias potential, generating a series of I/V curves. The data generated by this instrumentation will further the understanding of nano-scale electronics and bring the vision of a nano-electronics revolution one step closer to reality.

## 2) Theory

### 2.1 Classical model of conductance

The classical atomic model of conductance in macroscopic conductors was introduced by Drude in 1900 *(*Serway*)*, before the development of quantum mechanics. In this model, the electrical conduction in a macroscopic sized metal is derived assuming a free electron gas within the lattice structure of a bulk solid. An electron in presence of an applied electric field experiences a force and is accelerated. This acceleration of an electron is described by the charge of an electron ($q$) multiplied by the electric field ($E$) and divided by the electron mass.

$$\vec{a} = \frac{q\vec{E}}{m}$$

The accelerated electron will eventually collide with the atoms of the lattice and scatter. The electrons, can only achieve a finite maximum velocity (drift velocity) between scattering events. Because of the periodic nature of the lattice there is an average time ($\tau$) between consecutive scattering events of an individual electron. The drift velocity can be expressed in terms of the electrons acceleration and the time between collisions.

$$\vec{v}_d = \frac{q\vec{E}}{m}\tau$$

The current density ($J$) may then be written in terms of the density of electrons per unit volume ($n$) multiplied by the charge of an electron and the drift velocity.

$$\vec{J} = nq\vec{v}_d$$

The conductivity is simply the ratio of the current density to the electric field. (*Serway*)

$$\sigma = \frac{J}{E} = \frac{nq^2\tau}{m}$$

Conductance of the metal is the conductivity multiplied by the ratio of the conductor cross sectional area ($A$) and the length ($l$).

$$G = \frac{nq^2\tau}{m}\frac{A}{l}$$

The conductance depends on the parameters of the material: electron density time between collisions and the effective mass of the charge charier. Furthermore, the conductance also depends on the geometric properties of the conductor: cross sectional area and the length.

### 2.2 Quantum Conduction in a Single Atom

When the dimensions of a conductor are reduced to an atomic scale, quantum effects dominate and the macroscopic geometric dependencies are no longer applicable. Consider the ultimate limit of small conductors, a single isolated atom.

By definition, the conductance is the current ($I$) per potential difference ($\Delta V$).

$$G = \frac{I}{\Delta V}$$

The current is defined by the amount of electric charge passing per unit time.

$$I = \frac{nq}{\Delta t}$$

And the potential difference (voltage difference) is the electrostatic energy difference per unit charge.

$$\Delta V = \frac{\Delta U}{q}$$

By combining these equations, the conductance can be expressed with the following equation.

$$G = \frac{nq^2}{\Delta U \Delta t}$$

Because a single atom is inherently a quantum system, the Heisenberg uncertainty principle applies. The uncertainty principle tells us that the product of energy change and time change must be greater than or equal to Planck's constant (*h*) (*Cohen-Tannoudji*).

$$\Delta U \Delta t \geq h$$

Furthermore, the exclusion principle dictates that a single atom conductor can have a conduction electron spin up and a second conduction electron spin down (*Cohen-Tannoudji*) Therefore, the conduction electron number for the single atom is $n$=2 and the conductance of the single atom can then be written with the following equation.

$$G \leq \frac{2q^2}{h}$$

In the ideal case, the uncertainty is minimized and the inequality vanishes. The conductance of a single atom is given by the conduction quantum equation (*Landauer*)

$$G_o = \frac{2q^2}{h} = 8x10^{-5}\Omega^{-1}.$$

Consequently, the ideal resistance of a single atom is

$$R = \frac{1}{G} = 12.9k\Omega\,.$$

According to the equation, an isolated atom has an ideal conductance quantum independent of the atom species. However, it has been observed that nano-scale conductance is not independent of species (*Agraït*)

**2.3 Effects of the Electrode Interface**

For a single atom, between two electrodes, the conductance is determined by the quantum of conductance plus the geometry of the electrode interface and the bonding structure. Electron scattering occurs at the interfacial boundary and results in reflection and reduces the transmission through the conductor. Therefore, to more accurately describe the conductivity, the quantum conductance is scaled with the transmission probability (*T*) (*Ciraci*)

$$G = \frac{2q^2}{h}T\,.$$

Mathematically, the transmission probability (*T*) is the trace of the product of the transmission matrix (*t*) and its conjugate ($t^*$). Therefore, the most general form of single atom quantum conductance is *(Ciraci)*

$$G = \frac{2q^2}{h}Tr(t^+t)\,.$$

### 2.4 Multi-Atom Quantum Conductance

According to the classical model of conductance for a macroscopic conductor, the conductance increases linearly with the cross sectional area and falls as the inverse of the length. This model was derived form the average time between electron lattice collisions, and hence depends on the mean free path between scattering events (*Serway*).

The geometric dependence of nano-conductance must be different than that found in macroscopic conductors. Macroscopic conductance depends on the mean free path between electron scattering events. However, nano-conductors are smaller than the mean free within the bulk of the same material and charge carriers propagate without losing momentum. This is considered the ballistic electron transport regime and at this scale, the conductance does not have the classical length dependence *(Agraït).*

The conductance through a multi-atom nano-conductor is quantized with respect to the cross sectional area. *(Ciraci).* Each atom in the cross section contributes a quantum unit $G_0$ to the conductance. If the cross sectional area is changed the conductance will change accordingly in a stepwise manner.

### 2.5 Additional Physical Considerations

The theory of quantum conduction presented in this chapter, describes a simplified ideal metallic nano-conductor. It is a useful illustration but does not take into account the non-idealities, which may affect the conductance. For example, the theoretical ideal conductance is independent of the metal species. However, different metals may have

various oxidation layers, which affect the conductance (*Schmidt*)**.** Also, the theory depends on the assumption that momentum is not exchanged between the electrons and the atoms and this assumption may not always be valid.

## 3) Experimentation

The experiments were made using a piezo-driven break junction device (nano-press). The break junction device held the electrodes in the correct position to nanometer precision. The position was measured with an air gap capacitor and an ADE 481 gauge, which sent an analog signal into a DSM piezo-server. The piezo-server had a digital knob, which was used to set the position of the electrodes. After setting the position of the electrodes the server would maintain the position using the analog feedback signal from the ADE 481 gage. Measurements were made using a transimpedance amplifier, which would apply a bias potential and convert the resultant current into an analog output potential. The output potential was converted to a digital signal and recorded on a computer.

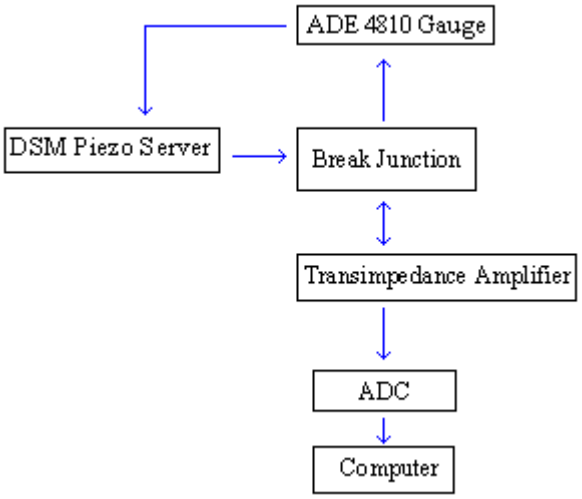


Fig 3.1 Block diagram of the experimental system.

### 3.1 The Break Junction Press

The break junction press is grounded and sits on a piece of conducting foam on a large optical table to reduce vibrations. It has a moveable piston, which is controllable with sub-nanometer precision. The

piston pushes a flex structure on which electrical contacts are mounted. As the piston moves upward it breaks the electrical contact and as the piston returns, the contact is reformed as shown in figure 3.2. Through careful positioning, a nano-contact with a width of tens of atoms or even a single atom can be formed.

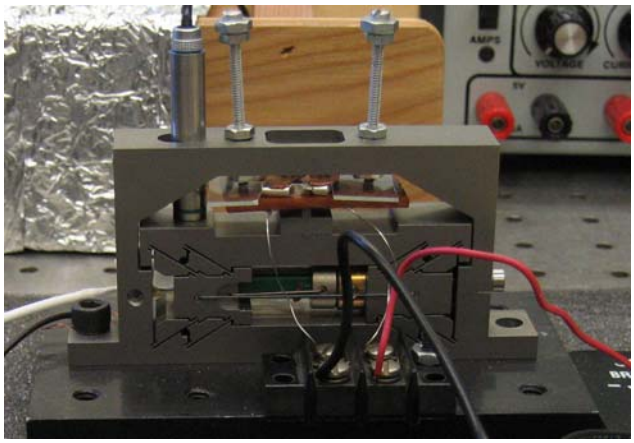

Fig 3.2 Break junction press with blade junction

The piston of the nano-press piston is driven with a piezo-electric crystal and has a full range of 40μm. The movement is controlled by manually turning a knob on the Dynamic Structures and Materials (DSM) SA-100 linear piezo-server amplifier, which applies a bipolar DC potential up to +/-90V.

### 3.1.1 Coarse Adjustment Modification

In early experiments it was often difficult to configure the sample in the middle of the piezo range. Experiments would fail because the break point would not occur within this 40μm range of the press. To eliminate these difficulties, two adjustment screws were added to the nano-press.

The adjustment screws push the flex the structure from the top without affecting the position of the piston.

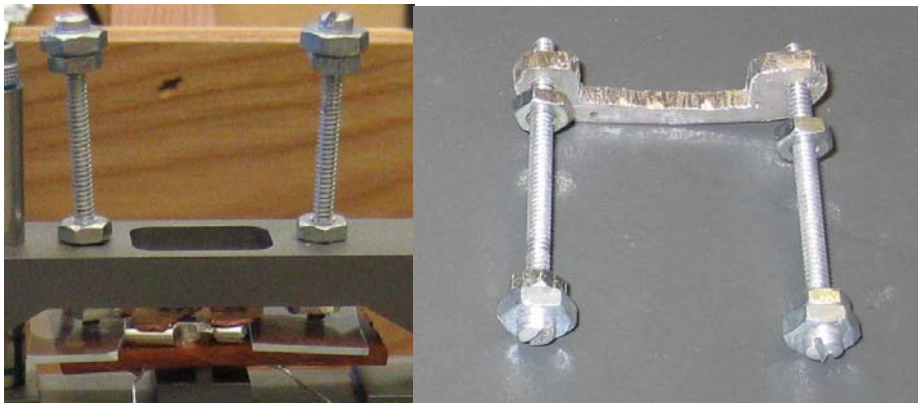

Fig 3.3 Adjustment screws

To fabricate the adjustment screw structure, two small bolts pass through the two holes on the top of the press. The bolts are held in place on the bottom with a piece of threaded aluminum sheet metal. The screws can be tightened so that they push against the glass on the flex structure holding it in place with compression and allowing a wide range of flexing.

Before each investigation, the piezo is set to the center range of its range. Then, the screws are adjusted and the conductivity is monitored. The adjustment screws can bring the electrodes within a micron of the desired position. When the desired position is achieved, the bolts can be locked in place with two locking nuts on the top of the press. The course adjustments worked so well that quantum conductivity was observed while making the adjustments by hand!

### 3.1.2 Position Sensor and Gauge

An ADE 2805 air gap capacitor probe with a 50μm range is mounted to the press. It is used to measure the position of the piston to nanometer precision. The ADE 2805 capacitor probe is connected by a coax cable to an ADE 4810 gauge instrument, which detects small changes in capacitance when the piston is moved. The probe and gauge are set such that a 1nm movement will cause a 400μV change in the gauge output potential, within a +/- 10V range. The position sensor measures the piston position and does not directly measure the electrode position.

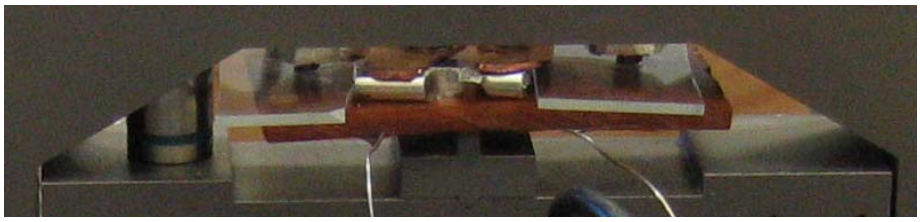

Fig 3.4 ADE 2805 air gap capacitor probe (left)

Experiments reveled that the press operator's proximity to the coaxial capacitor probe cable influenced the position measurements. Because the DSM piezo-sever is designed to use the ADE gauge output potential to maintain the position, it would change the position of the position to counter the changes in capacitance. This would cause the physical junction position to be unstable while the position gauge data appeared constant. This situation renders accurate data acquisition impossible. In addition the cable could not be in electrical contact with the system ground or false readings and corrective movements would result. To minimize these adverse effects, the cable was placed in an insulated

box to keep its capacitance constant. The box was then placed inside a conductor to electrically shield it. This helped, but led to the realization that the gap can only remain stable on short time scales with this setup.

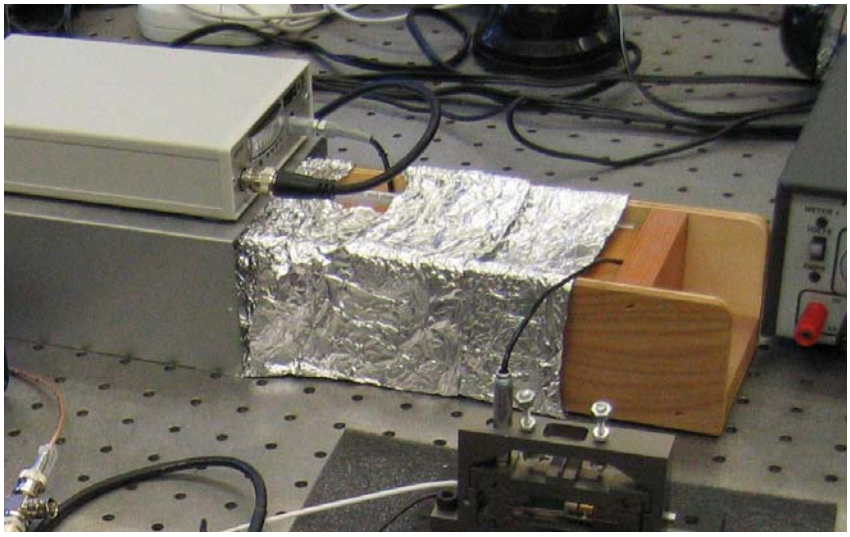

Fig 3.5 Insolated capacitor probe cable box

### 3.1.3 Gold Wire

The properties of gold metal make it a good choice for nano-conductor fabrication and experimentation. Gold, which does not oxidize with exposure to the environment, reduces the risk of contamination due to surface impurities caused by oxidation.

The initial experiments used thin gold wire mounted to a plastic flex structure with screws or a thin gold wire mounted to a glass flex structure with epoxy (*Ketter*). Later experiments used an improved glass flex structure design. A glass microscope slide is cut to size and two strips of copper tape are attached with a small gap between them. Soldering flux is applied and a 0.005” gold wire is attached to one side. Tension is then

applied to the wire by clamping hanging weights to it and then the other side is soldered in place. The wire is then shaved into two sharp points using a razor blade. A needle is used manipulate the wire ends such that they barely make electrical contact. The contact can be detected with the chime function of a meter or the break junction circuitry. Small gage connecting wires are attached to each of the strips of copper foil. One of the connecting wires is a ground and the other connects to the junction bias and current measuring circuitry. To reduce the possibility of interfering with the position gauge, the grounded side of the flex structure is placed next to the air gap capacitor.

This structure worked well. However, the main drawback with using this method was accidental breaking of the glass when tightening the course adjustments screws. It was also easy to over cut the gold wire preventing any electrical contact. To make contact, most of the gold wires required extensive manipulation with the needle after the flex structure was in place on the nanopress.

### 3.1.4 Tin-Silver Blades and the Second Flex Structure Design

Several improvements were made to the flex structure, and the electrodes were made with tin-silver solder. This material was initially chosen because it is easy to work with, and low cost, allowing rapid prototyping. It also had the added benefit of being an important material for the electronics industry, which is actively fazing out the use of lead-based solder.

The glass flex structure base was replaced with a stiff piece of flexible plastic circuit board material. Two small glass shims are used between the flexible base and the coarse adjustment bolts for a more stable mounting. This new structure proved to be much more rugged and eliminated the frustration of breaking the base of the flex structure. This choice of material may not be suitable for high vacuum work, but is otherwise ideal. It has holes in it allowing bolts to be placed through it to hold the solder electrodes in place. Small pieces of copper are cut and are used as mounting washers. Together with a nut they hold perpendicularly opposed solder blade electrodes in place. The bottom of the structure has two strips of copper foil which make electrical contact with the mounting bolts and the connecting wires are then soldered to the strips.

The perpendicularly-opposed electrode blades create a small point contact region which is ideal for these experiments. The blades are fabricated by flattening the end of a solder wire in a vice. The flattened ends are cut to form a sharp knife-edge using a razorblade and a glass cutting board.

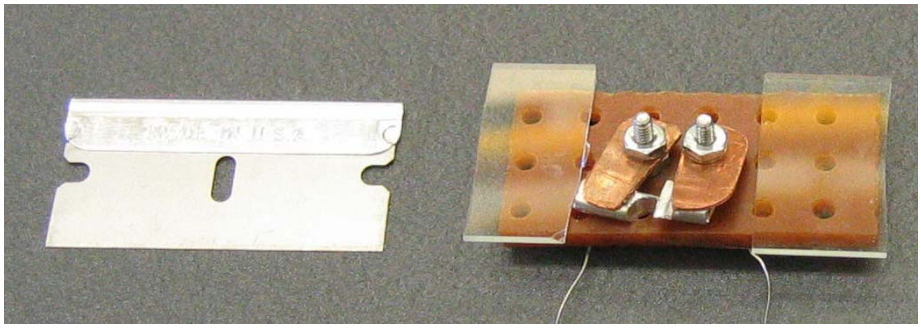

Fig 3.6 Tin-silver blade junction and flex structure

### 3.1.5 Gold Blade Flex Structure

After making a prototype blade structure with tin silver solder, a second flex structure with pure gold. The procedure was similar; however, the blade size was reduced. Glass sheets cover the copper tape in on the gold flex structure providing electrical insulation and firm contact with the press.

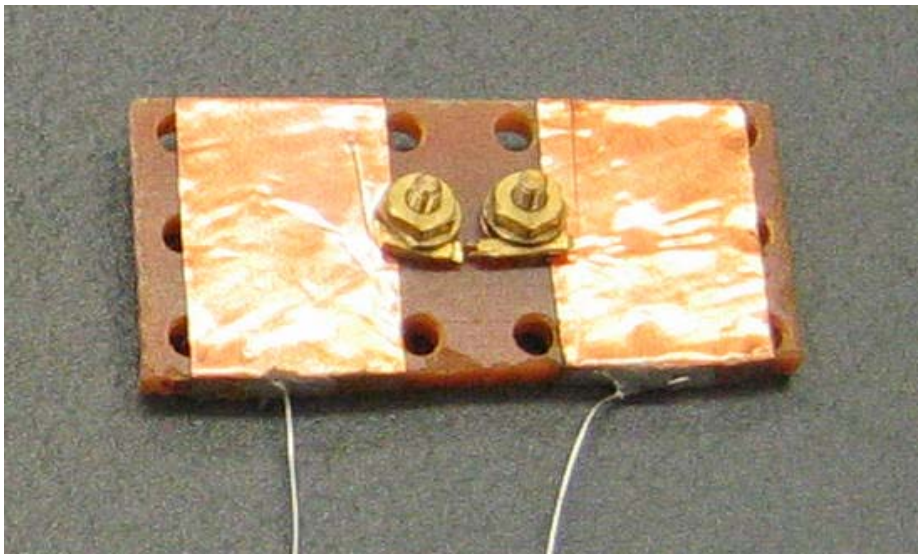

Fig 3.7 Gold blades junction and flex structure

## 3.2 Transimpedance Amplifier.

Quantum current measurements were taken with an operational amplifier circuit, which is shown in fig 3.2. The op-amp is a Texas Instruments TLC27L7, powered with a +5V external DC power supply. The contact bias is achieved using a potentiometer as a voltage divider at the non inverting input. This causes an equivalent bias at the contact or nano-conductor induces a current through the contact. The amplifier

converts the current to a potential which is scaled by the feed-back resistor. This potential is then recorded by a computer as a function of time. The resultant potential could then be monitored with a meter or the EPP Data Logger built by Tim Taylor of the OSU Physics Department.

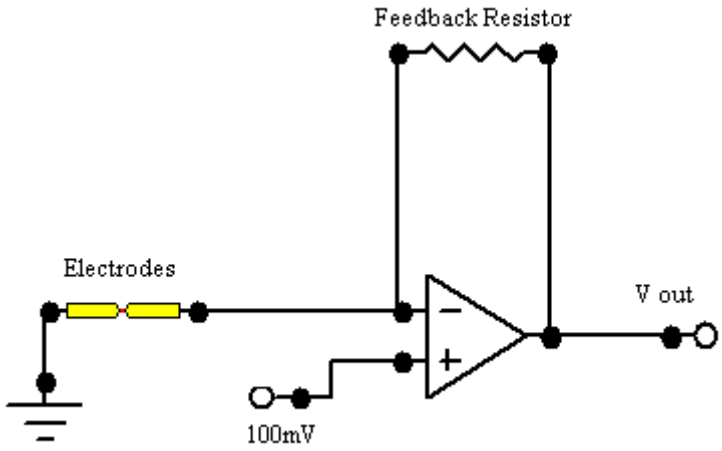


FIG. 3.8 Schematic of transimpedance amplifier

The current to potential amplifier circuit may be easily understood using the rules for an ideal operational amplifier:

1) The current flowing into either op amp terminal is zero.
2) The voltage difference between the inverting and non-inverting terminals is zero

A small positive potential of 100mV is applied to the non-inverting input ($V_+$) of the op-amp. From rule number two, the potential difference across the junction is equal to $V_+$. Ohm's law states that the current across the junction is equal to the potential over the junction resistance. Rule number one and conservation of charge mandate that this same current

must have traveled through the feedback resistor. Using Ohm's law again, the potential difference between the output and inputs of the op-amp is simply the product of the current and the feedback resistance.

$$\Delta V = V_{out} - V_{+} = IR_f$$

An expression for the current can be written as

$$I = \frac{\Delta V}{R_f}.$$

With both the bias and the current across the junction known, the resistance and conductivity may be determined theoretically using Ohm's Law.

$$R_{junction} = \frac{V_{+}}{I} = \frac{V_{+} R_f}{V_{out} - V_{+}}$$

$$G_{junction} = \frac{1}{R_{junction}} = \frac{1}{R_f}\left(\frac{V_{out}}{V_{+}} - 1\right)$$

In practice the conductivity was determined experimentally rather than theoretically. 13kΩ resistors were placed in parallel at the input of the transimpedance amplifier and the output potential was measured as a function of the number of resistors. The results were plotted in MS Excel and a line was fit to the curve. The lines were a near perfect fit and the slope of the lines provided the potential to conductance conversion factor used in the conduction plots.

### 3.3 Data Acquisition System Development

There are many limitations associated with the data acquisition and control system. Slight fluctuations in position sensor capacitance cause the control system to change the position. In addition, the position is changed to counter the capacitance feedback, no change is observed on the gauge. Vibrations and thermal effects also contribute to the unsuitability of the gap. There are also dynamics occurring on a time scale shorter than what can be currently measured.

A new system was designed to complete high-speed experiments within the short time for which the gap is stable. The system concept is completely automated, with no capacitive feedback dependence. The concept is to rapidly sweep a range of electrode spacing and for each position of interest the contact bias potential is ramped. Then, a current vs. potential as a function of time curve is recorded.

The transimpedance amplifier and a cypress CY7C68013A microcontroller form the core of the new system. The microcontroller has three 8 bit I/O ports and is connected to a host computer through a high speed USB cable. To maximize the speed, most of the programming was written in assembly code (by Joe Magner), compiled into binary firmware and downloaded directly to the microcontroller where it is executed. The remainder of the software, where speed is not a factor, will be written in Python (by W. Hetherington). The data is streamed back from the microcontroller to the host computer where it is plotted using python.

The microcontroller is mounted to a printed circuit board developed by Connor English, an OSU physics student. The circuit board was designed for use with a surface mounted AD976 high speed, multiplexed, analog to digital converter. The AD976 converts the incoming data with 16 bits conversion at a rate of 200KSPS. The AD976 is a multiplexed output parallel converter, which uses 8 bits for data and an additional 4 bits for control. This means that there are only 12 bits left on the microcontroller for all the control circuitry. For this reason it was decided to use DG413 CMOS analog switches to address MCP4822 Digital to Analog Converters. This choice makes the programming more difficult but accomplishes the task with the remaining I/O pins. The pin assignment of these devices is provided in the appendix.

The microcontroller operates with a 12 MHz clock and an instruction takes 4 clock cycles. The instructions are then completed at a rate of 3 MHz or 333ns per instruction. The digital to analog converter requires 32 instructions (at 333ns per instruction) and can out put a number approximately every 11 microseconds. An analog to digital conversion takes approximately 5 microseconds. By summing the times it is determined that the system requires a at best a minimum of 16 microseconds per data point. Assuming that each current vs. potential plot will have 100 data points then it will require 160microseconds to collect the data. This means that the new system will have an approximate ideal sampling rate of 6.25 thousand I/V plots per second. It is anticipated that the actual sampling rate will be slower and that this value is only an order of magnitude approximation.

| | |
|---|---|
| $12MHz \times \frac{1}{4cycles} = 3MHz$ | Instruction rate |
| $333ns \times 32instructions \approx 11\mu s$ | DAC conversion time |
| 5µs | ADC conversion time |
| 11µs + 5µs = 16µs | Time per data point |
| 16µs x 100 = 160µs | Time per I/V set |
| 6.25KHz | I/V sampling rate |

### 3.4 Thermal Expansion Concept

A possible future direction for this research is to develop a differential thermal expansion type break junction. A frame structure, consisting of thin insulated section between two opposing metallic horseshoe sections, could be mounted to a thermoelectric device. A metal sample could then be clamped within the frame structure like a string in a harp. As the system is heated or cooled small differential thermal expansion or contraction could create a nano-contact in the metal sample.

Here is an example of how a thermal break-junction system could work. The goal would be to pull a gold wire into an atomic scale contact. Experiments have shown that a 500nm wide wire of gold will have a ductility of 2% to 4.5% when slowly pulled (*Bateson*). Here we will assume a maximum ductility of 5% for the thin gold wire to be safe. Now the gold wire is mounted to the break junction frame structure. The wire is of length *L* and the center of the wire has a section with a much smaller section of length *l* and an ultra thin diameter of 500nm. Defining the differential coefficient of expansion (α) as the difference in the coefficient of expansion of the gold and the break junction structure.

$$\alpha \equiv (\alpha_{structure} - \alpha_{gold})$$

If the wire is much thicker than the 500nm thin section it can be assumed that the pulling will only change the length of the thin section. And this change in length of the thin section is equal to the differential change in length, between the wire and the structure, which is defined as the change in the structure length minus the change in the gold length.

$$\Delta l \equiv (\Delta L_{structure} - \Delta L_{gold})$$

For breaking to occur, we set the differential change in length equal to the length of the narrow section of gold times the maximum ductility.

$$\Delta l \approx 0.05 l$$

The full temperature range with which we will be working is ΔT. Now putting it all together we get an expression for the geometry in terms of the temperature range.

$$\frac{l}{L} \approx 20 \alpha \Delta T$$

The thermal expansion break junction concept seems quite feasible. The work found in the literature search did not show any use of this method. Nano-contact formation with differential thermal expansion could very well make an interesting and original research project.

## 4) Quantum Conduction Data and Analysis

### 4.1Tin-Silver Quantum Conductance

Several experiments were conducted where the blades were slowly moved closer together until conduction began, at which point the position was held constant. The bias potential was held at a constant 100mV and the resultant current is measured with the transimpedance amplifier. The position was held constant to minimize any digital movements of the press, which could be mistaken for quantum effects.

The data was converted from current and potential to conductance and plotted in units of $G_0 = 1/13 m\Omega^{-1}$, the approximate theoretical quantum conductance. The conductance scale of $G_0$ is also the approximate number of parallel atoms at the contact. The x axis represents time in units of 10ms.

The data in fig 4.1 shows a stepwise increase in the conductance. There may be a slight vertical offset, but the steps size appears promising. The plot appears to be consistent with the theory of quantized conductance.

As noted earlier, once the conduction began at about 450ms the position was held constant. However the conductance continues to increase, possibly the result of a positive feedback process and there are no steps of decreasing conductance. One possible cause is that there is significant Joule heating and a high current density causing an electromigration of atoms from the upstream side into the nano-contact. As we will see in the section on electromigration, a current limiting

resistor can be added to reduce the current after physical contact is made. Thus, ultra thin nano-conductor which is stable for time scales on the order of seconds may be created.

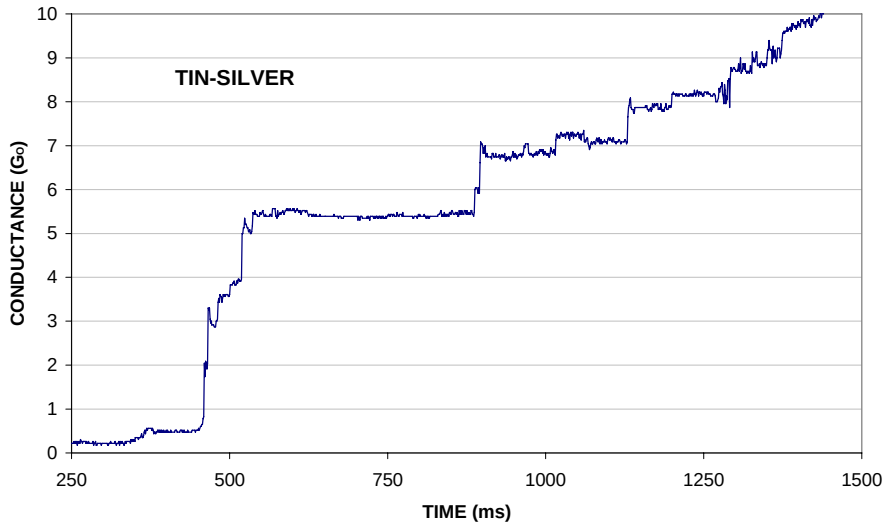


Fig. 4.1 Increasing conductance steps

Several experiments were also conducted where the tin-silver blade contact was pulled apart under a constant 100mV bias. The position was held constant once the decrease in conductance begins so the steps are not the result of the digital press movements. In contrast to the example in the prior section, the observed conductance decreased with the appearance of an exponential decay, which is shown in Fig. 4.2 . Interspersed within the decay curve are what may be quantum steps in the conductance. The size of the steps is on the order of $G_0$, which is in agreement with the theoretical expectations.

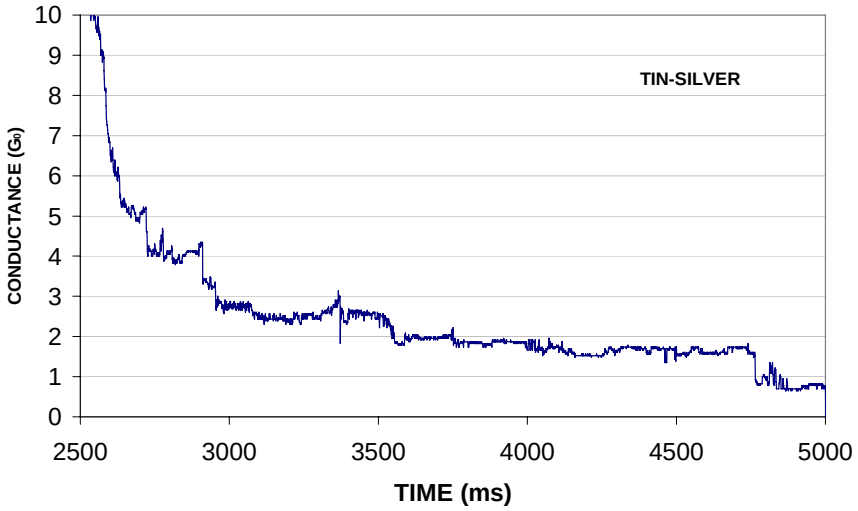


FIG 4.2 Decreasing conductance steps

All of the conduction experiments have been preformed under DC conditions. Therefore, nothing is known about the complex impedance of the nano-conductors. There must be some kind of phase dependence associated with these nano-conductors. Unlike resistance measurements, measuring the phase dependence of a nano-conductor is inherently difficult. The nano-conductor is not an isolated system, the electrodes connecting wires and measurement circuitry all need to be taken into consideration.

The resistance of a nano-conductor is much larger than the resistance of the bulk metal it is in contact with. This means it possible to make accurate and specific conductance measurements of the nano-conductor. However, the inductance and capacitance is considerably larger in the bulk and connecting hardware. Therefore, phase measurements would be difficult and were not investigated in this research project.

### 4.2 Hysteresis

Hysteresis tests were conducted with the tin silver blade junction. The transimpedance amplifier applied a constant 100mv bias potential at the solder blade contact and measured the resultant current. In this experiment the open position is defined at zero conductance and the closed position is defined as a conductance greater than ten quantum units.

The observed distance between the open gap and closed contact positions ranges between 90nm at best to 1840nm at worst, which is shown in Fig4.3. It is important to note that the distance measurements refer to the piston position and are not direct measurements of the electrodes. The absolute value of these positions tended to drift linearly with each successive trial. After eight trials the mean position value had drifted 2105nm.

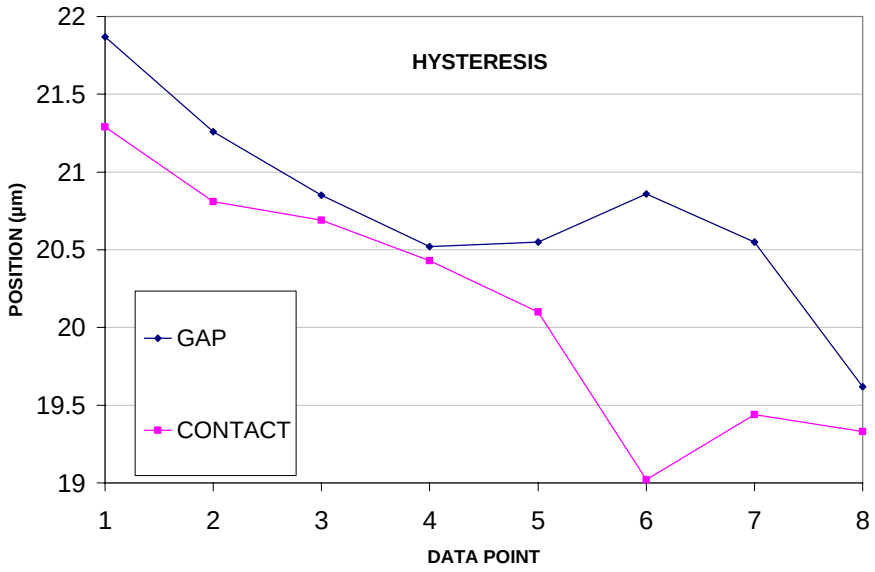


Fig. 4.3 Hysteresis in tin-silver contacts

### 4.3 Gold Quantum Conductance

Experiments have been conducted using the gold blade structure. The bias was held at a constant 100mv bias and the electrodes are held at a constant separation once conduction begins. Unlike tin-silver, for gold, only steps of increasing conductance were observed. A staircase of decreasing conductance steps or a smooth decay of conductance, which was expected for these experiments, was not observed. The gold always increased in conductance without any of the fuse like behavior seen in tin-silver.

Figure 4.4 shows the conductance verses time for a gold nano-contact. The steps appear to be consistent with the theory of quantized conduction.

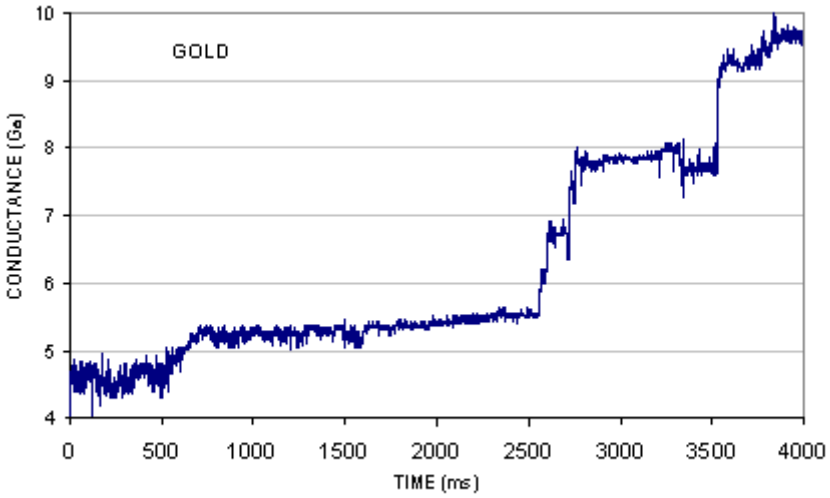


Fig 4.4 Steps of increasing conductance observed in a gold nano-contact with the electrode blades held at a constant position.

### 4.4 Quantum Conductance Data Analysis

Three datasets, such as that pictured in Fig 3.4, of increasing conductance for both gold and tin-silver were used to create a histogram for analysis. The step size is scaled in terms of quantum conduction units ($G_0$). Although, because of the subjective nature of determining what constitutes a step, more data sets are needed to for a complete analysis, a trend is evident here. The most probable step size observed here is $1G_0$ for both gold and tin silver. This is the value of a single atom moving into the neck of the conductor. Furthermore, the frequency of the step size falls off quickly with G. For both data sets, steps of $4G_0$ or greater were not observed. However, large steps of 8 or more would have been out of the range of the data acquisition system resulting in a saturation condition.

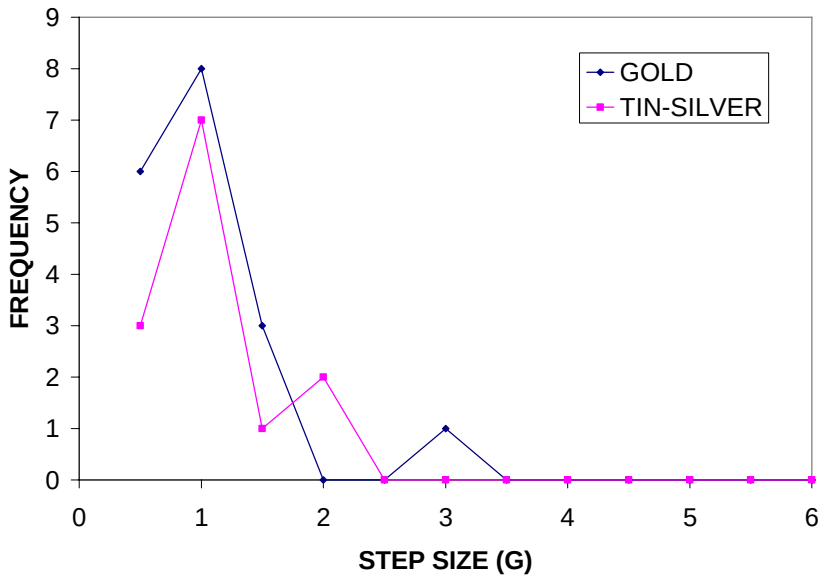


Fig 4.5 Histogram for gold and tin-silver blade electrodes

### 4.5 Tunneling at Gold Wire Electrodes

Initial junction experiments, using gold wire, did not appear to show any quantized effects. The gap conductance appeared to change as a function of position in a continuous manner. Later it was discovered that the current to voltage amplifier was not calibrated correctly. The readings were about 100 times more sensitive than expected. So, all the measurements were of the tunneling current and physical contact was not made. The error in calibration calls into question the gold wire data sets that had a stepwise appearance. Without the exact calibration, the measured values and established values may not be compared for these data sets.

After solving the calibration issue, the conductance appeared to be continuous at values where quantum steps were expected. After several experiments it was hypothesized that this is the result of the wires moving out of alignment. The wire tips would miss and the wires would be parallel, resulting in a large amount of tunneling current between the wires.

Sometimes the data appeared inverted. It is hypothesized that there were extrusions or whiskers on the side of the wires. If the wires are parallel and have extrusions, then it is reasonable that the wires could be hooking and making physical contact instead of separating.

## 5) Electromigration

Electromigration is the movement of metal atoms caused by electron flow and temperature. In electromigration, momentum is transferred form the electron current to the metal atoms, through electron scattering. Electromigration effects occur on the down stream direction (*Hawkens*).

The work with electromigration presented in this thesis came about by accident. The original objective was to carefully "spot weld" the electrodes together on a microscopic scale, so that they could be pulled slowly and drawn into a nano-contact with the break junction press. However, it was discovered, that with a sufficient potential across the electrode gap, that a conduction path is formed. This formation occurs without having to change the position of the electrodes with the press. Therefore, it is assumed that, a conduction bridge forms between the electrodes a result of electromigration. This assumption is consistent with the observations of other researchers, found in the literature search.

### 5.1 Nano-Conductor Formation

Nanoscopic metallic bridge formation using electromigration was successfully demonstrated using opposing tin-silver electrode blades. The blade edges had an approximate separation gap of tens of nanometers. The separation was achieved by separating the blades until electrical contact is broken and then decreasing the separation distance as much as possible without making contact. This is a delicate process and some intuition is needed because of the hysteresis inherent in the system. The blades are then held at a fixed position and an increasing DC bias potential is slowly

applied. The current and potential measurements are made by hand with multimeters.

In the experiment shown in Fig 5.1, current was negligible for bias potential less than 920 mV. At this point a nano-bridge formed between the electrode blades (data points 5 and data point 6). A 20KΩ current limiting resistor on the power supply reduces the potential when a conduction path is formed preventing excessive power dissipation. The after the formation of the conduction bridge the bias fell to 65mV with a current of 61microamps (data point 6).Using Ohm's law the resistance of the conductor is found to be 1.1KΩ.

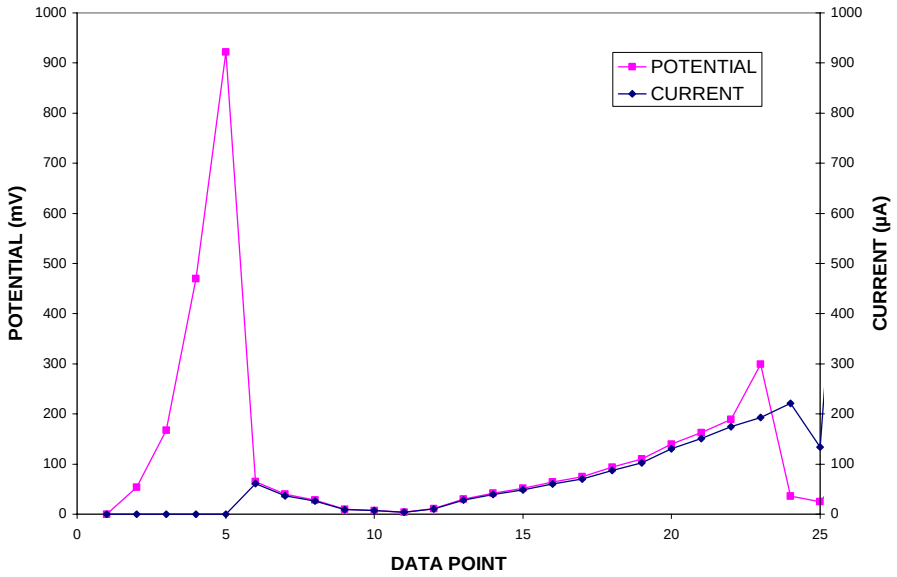


Fig 5.1 The formation of a 1.1KΩ nano-bridge conductor between tin-silver electrode blades.

The current was measured as a function of bias potential (data points 6 through 22) and the conductor had a linear current vs. potential relationship as shown in Fig 5.2. The conductivity of the wire was approximately $G=12G_o$ which corresponds to a cross sectional waist of only 12 atoms.

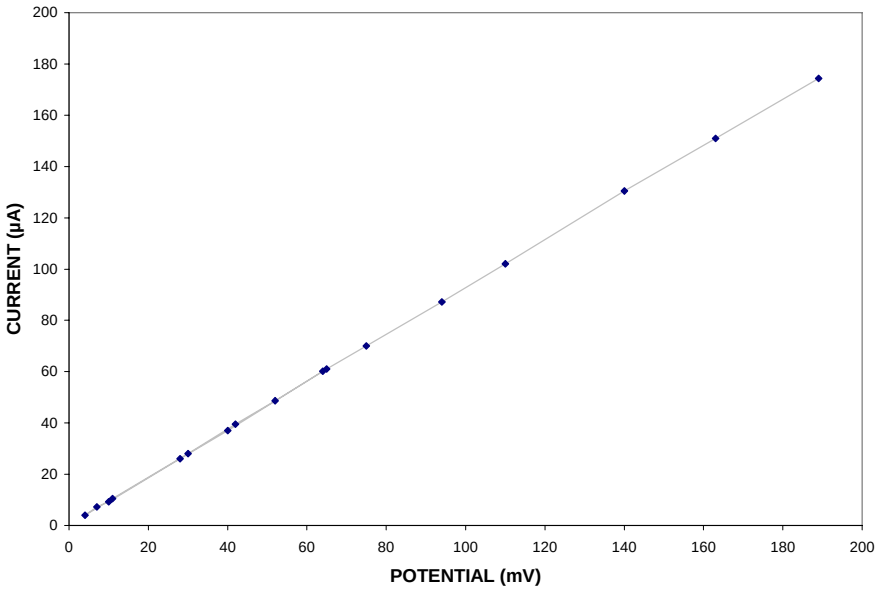


FIG 5.2 The current as a function of bias potential for the nano-bridge formed between electrodes held at a constant position. The resistance is 1.1Ω and the conductance is $12G_0$.

The conduction bridge was remarkably stable for biases up to 289mV, a current up 174.3 micro amps and a power dissipation of 50μW. Power dissipation in excess of this caused a second formation event. The resulting conductor had a greater conductivity which could be attributed to a thicker waist (data points 23 and 24).

Additional electromigration tests, such as that shown in Fig. 5.3, were preformed using the solder blades. The blades were held at a constant position with a separation distance believed to be on the order of tens of nanometers. The bias was slowly increased and the resultant current was less than the 0.1μA sensitivity of the meter. When the bias exceeded 860 mV, a quantum tunneling current on the order of 20 micro amps was observed (data point 6). Bridge formation occurred for a bias near 1100mV. At the time of formation the approximate power dissipation

at the gap was 2.2μW. After formation the current limiting resistor dropped the voltage to 93mV with a current flowing through the nanowire is 90 micro amps (data point 8). The current vs. potential characteristics are stable and linear with a resistance of 1.0KΩ ($G=13G_o$). According to quantum conduction theory the measured resistance indicated a minimum waist of 13 atoms for this conductor. The conducting bridge remained stable until the bias exceeds 194mV with a current of 190μA and a power dissipation of 37μW. Then a formation event occurred (between data points 12 and 13). At that point the current vs. potential characteristics became linear again with a resistance of 130 ohms ($G=100G_o$) and a minimum waist of approximately 100 atoms (data points 13 through 22).

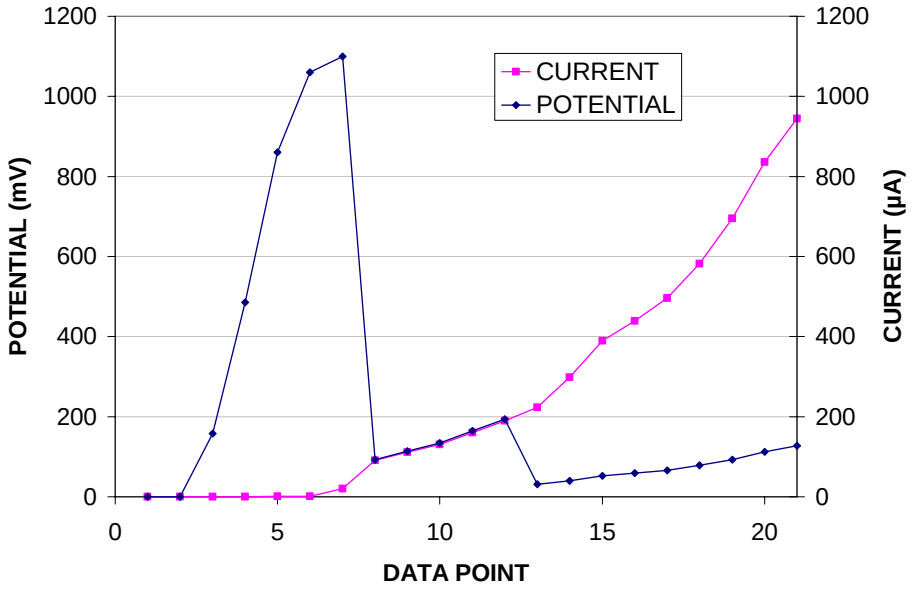


Fig 5.3 The formation and reformation of nano bridges from electromigration between two opposing tin silver blade electrodes held at a constant separation.

The I/V characteristics for the two conduction bridges are shown in fig 5.4. The slope of the lines indicates the conductance in $m\Omega^{-1}$. The second bridge has a much steeper slope, which is expected, because the

conductivity increases with thickness. So, as expected, the wire bridge is thinnest after the initial electromigration formation and becomes thicker after each additional formation process.

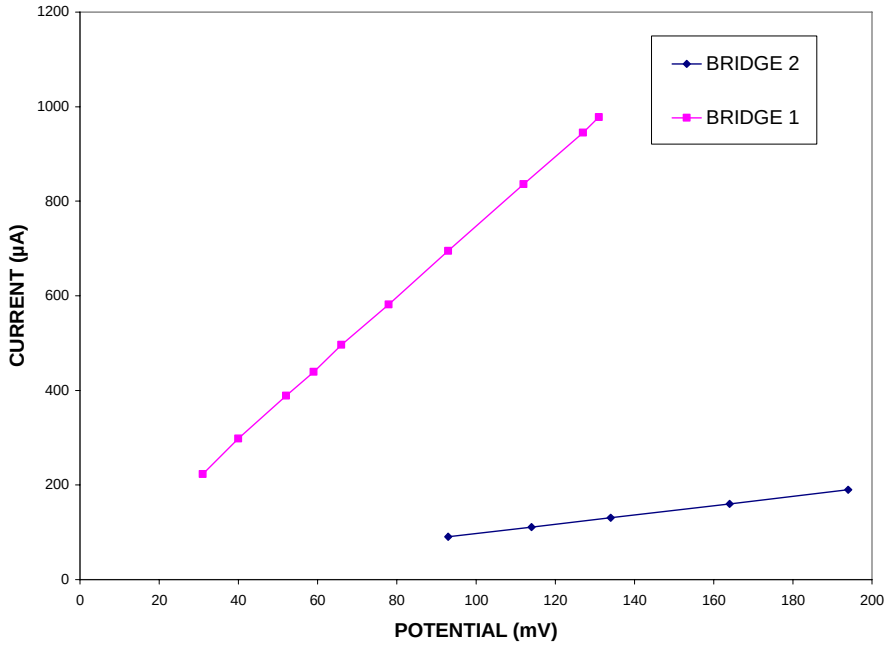


FIG 5.4 The current as a function of potential for tin-silver nano-bridges formed in Fig 5.3. The second formation leads to a steeper slope or greater conductivity as expected. The slope shows the conductivity in millsiemens and the measured resistances are 1KΩ and 130Ω.

Amazingly, the nano-bridges shown in this section were stable with time. It took about a minute to conduct these experiments. This type of stability was never seen before the introduction of the current limiting resistor.

### 5.2 Thermal Model

The experiments presented in the previous section started as an attempt to weld the electrodes together. It was hypothesized that the electrodes could be spot-welded together on an ultra small scale. The electrodes are brought together under a sufficient potential such that at or

near contact there will be an electric discharge or arcing. The discharge of electrical energy results in localized heating melting the small contact region of the electrodes. A current limiting resistor immediately causes the potential to drop and the melted metal quickly solidifies. Essentially, this is a capacitive discharge using the capacitance of the electrodes. The power supply is needed to maintain the bias potential even as current leaks between the electrodes as a result of tunneling.

Let's use this approach to analyze the observations made in the experiments. This power dissipated at the contact is the product of current and electrical potential.

$$P = IV$$

In the experiment shown in fig 5.1C the bias was1.1V before the first formation event. At this potential there was a tunneling current of 20μA with a power dissipation of 22μW.

$$P_0 = 1.1V \times 20\mu A = 2.2\mu W$$

This is the maxim power dissipated in the gap before a bridge formed. At a slightly larger power the bridge formed between the electrodes. The bridge is not destroyed until the power exceeds 37μW which is the approximate upper power limit for the first bridge.

$$P_1 = 194mV \times 190\mu A = 37\mu W$$

From the power limits a simple thermal calculation can be made to determine the approximate size of the conductor, which will melt. For simplicity, and because nothing is known about the true geometry, the contact region will be modeled as a solder cube. The electrical power dissipated at the contact is converted to thermal power and that thermal power is conducted through the contact according to the equation

$$Power = \frac{\Delta Q}{\Delta t} = KA\frac{\Delta T}{\Delta X}.$$

Where K is the thermal conductivity for 50/50 solder from the 67th edition of the CRC Handbook of Chemistry and Physics, A is the cross-sectional area ($A=\Delta X^2$), $\Delta X$ is the length and $\Delta T$ is the difference between the melting temperature of the solder electrodes and room temperature.

Solving for the length of the hypothetical conducting cube we get

$$\Delta X = \frac{Power}{K \times \Delta T}.$$

Using the maximum power value for the cubic conductor, the size is

$$\Delta X = \frac{P_1}{K \times \Delta T} = \frac{37 \times 10^{-6} W}{\left(80 \frac{W}{m^{o}C}\right) \times 200^{o}C} = 2.3 \times 10^{-9} m.$$

So, the hypothetical cubic conductor has dimensions of 2.3nm which is a reasonable scale. The calculations are admittedly an over simplification and the exact geometry and physics of the contact is unknown. However the calculations show reasonable limits for the expected size of the contact.

## 5) Conclusions

The instrumentation has improved significantly as a result of this work. A more sophisticated break junction system was developed which eliminates many of the difficulties encountered at the beginning of this project. These difficulties included high tunneling currents caused by the electrodes failing to make contact at the ultra sharp tips. This problem was solved by using new electrode blade geometry instead of opposing tips. The system was further improved by using the property of electromigration to grow the nano-conductors between the blades.

Using the improved system it was demonstrated stable, ultra-small conductors could consistently be formed between the electrode blades. Conductance measurements and theoretical thermal calculations indicate that the conductors were on the scale of nanometers. The nano-conductors had quantum electrical properties including size dependent conductance steps consistent with the theory of quantized conduction.

The nano-conductors formed with electromigration appeared stable on a time scale of minutes. The data indicates that these conductors have waists as narrow as 12 or 13 atoms. For small currents, less than approximately 200 micro-amps, the potential was proportional to the current. When the current exceeds this threshold the conductance would increase indicating a widening of the cross-section. Experimental work indicates that at the 200 micro-amp threshold the waist changed from approximately 13 atoms to 100 atoms. After the conductance change, the conductor was stable and had a new, proportional current and potential relationship.

A major limitation of this investigation so far is that electrical properties of the bridges were studied using multi-meters and the data was recorded by hand. Although excellent data was generated, the dynamics of conductor formation was occurring at faster time scale and could not be recorded by hand.

My final contribution to this project was to design a new high-speed data acquisition and control system to be used in future research of the conductor formation dynamics. The system is designed to rapidly scan the nano-conductoor as a function of position and bias potential, generating a series of I/V curves. The new system will capture new high-speed electrodynamics and it is anticipated that the data generated by this instrumentation will further the understanding of nano-scale electronics.

**References**

Agraït, Untiedt, Rubio-Bollinger, and Vieira (2002)
Onset of energy dissipation in ballistic atomic wires
Physical Review Letters, vol. 88, Issue 21

Bateson (2004)
Characterization of strain rate dependence in the mechanical behavior of gold thin films
University of Virginia, Mechanical and Aerospace Engineering document

Ciraci, Buldum and Batra (2001).
Quantum effects in electrical and thermal transport through nanowires
Journal of Physics: Condensed Matter 13

Cohen-Tannoudji, Diu, Laloe (1977)
Quantum Mechanics
Hermann and John Wiley and Sons ISBN 0-471-16432-1

Emberly and Kirczenow (1998)
Theoretical study of electrical conduction through a molecule connected to metallic nanocontacts
Physical Review B, Volume 58

Hawkins and Seguram (1999)
Test and Reliability: Partners in IC Manufacturing, Part 1
IEEE Design & Test of Computers July-September 1999

Ketter (2005)
Break-junction studies of current quantization
Oregon State University Physics Masters Project Report

Kornilovichl (2003)
Mechanically Controlled Breakjunction Progress Report
H.P. Dodument

Landauer and Imry (1999)
Conductance viewed as transmission
Reviews of Modern Physics, Vol. 71, No. 2

**References (continued)**

Sakaa and Ueda (2005)
Formation of metallic nanowires by utilizing electromigration
Department of Nanomechanics, Graduate School of Engineering, Tohoku University, Aoba-ku,
Sendai 980-8579, Japan

Schmidt, Martel, Sanstrom, and Avouris (1998)
Current-induced local oxidation of metal films: mechanism and quantum size effects
Applied Physics Letters, Volume 73, Number 15

Sen, Gulseren, Yildirim, Batra and Ciraci (2002).
Pentagonal nanowires: A first-principles study of the atomic and electronic structure.
Physical Review B, Volume 65

Serway and Beichner (2000)
Physics for Scientists and Engineers
Sanders College Publishing ISBN0-03-022654-6

Teverovsky (2003)
Introducing a new member to the family: gold whiskers
QSS Group Inc. /Goddard Operations
Internal Memorandum-NASA Goddard Space Flight Center